

Symmetry-preserving discretizations of arbitrary order on structured curvilinear grids

Bas van 't Hof* Mathea J. Vuiik†

August 26, 2021

Abstract

Mathematical descriptions of flow phenomena usually come in the form of partial differential equations. The differential operators used in these equations may have properties such as symmetry, skew-symmetry, positive or negative (definite)-ness. Symmetry-preserving methods are such that the discretized form of the continuous differential operator exhibits the same properties as the continuous operator itself. The use of symmetry-preserving discretizations makes it possible to construct discrete models which allow all the manipulations needed to prove stability and (discrete) conservation properties in the same way they were proven in the original continuous model. Furthermore, these methods allow a discretization of the continuous adjoint which is at the same time the discrete adjoint of the discrete forward model. Such adjoint models are not harder to code than the discrete forward model.

This paper presents a new symmetry-preserving discretization of arbitrary order on curvilinear structured grids. The key idea is to use mutually-adjoint sampling and interpolation operators to switch between the continuous and discrete operator. The novelty of this work is that it combines three important requirements for discretizations: first, the symmetry-preserving discretization is made for arbitrary order of accuracy; second, the method works for every structured curvilinear mesh; and third, the method can be applied to every continuous operator. This paper is the first in a series of papers that gradually extends the theory to a general approach.

Symmetry-preserving discretizations, Energy conservation, Mass conservation, Curvilinear grid

1 Introduction and motivation

Mathematical descriptions of flow phenomena usually come in the form of partial differential equations. The differential operators used in these equations may have properties such as symmetry, skew-symmetry, positive or negative (definite)-ness [25]. Proofs of stability and/or conservation properties, such as conservation of mass, momentum, and energy, can often be constructed using the symmetry and/or positiveness of the operators in the flow model [1].

Computer simulations of a flow phenomenon require the discretization of the flow properties, reducing the number of values needed to represent the flow state from infinite to some large finite number. In the resulting discrete model of the flow phenomenon, the differential operators have been replaced by difference operators. Unfortunately, not all properties of the differential operators are automatically inherited by their discrete approximations. The chain and product rules needed in the manipulation of nonlinear equations, for example, do not always work in discrete cases. Moreover, symmetry and positiveness may be lost in the discretization process, mass, momentum, and energy

*bas.vanthof@vortech.nl. VORtech, P.O. Box 260, 2600AG Delft, The Netherlands.

†Corresponding author. thea.vuik@vortech.nl. Telephone: +31 (0)152850125. VORtech, P.O. Box 260, 2600AG Delft, The Netherlands.

may not be conserved, aliasing errors can occur, and duality and self-adjointness of the differential operators may be violated [1, 10, 14].

The above difficulties play an important role when adjoint models are considered. Every (partial) differential model has an adjoint model, as does every (discrete) difference model. The adjoint model is needed in optimization problems and is often used to find solutions for seismic models [3, 19]. A big dilemma in optimization is often the choice between the (discrete) adjoint of the discrete forward model and the discretization of the (continuous) adjoint of the continuous forward model. Adjoint models of discrete forward models often lead to very complicated and inefficient computer code [3].

Symmetry-preserving methods are such that the discretized form of the continuous operator exhibits the same properties as the continuous operator itself [10]. The use of symmetry-preserving discretizations makes it possible to construct discrete models which allow all the manipulations needed to prove stability and (discrete) conservation properties in the same way they were proven in the original continuous model. Furthermore, these methods allow a discretization of the continuous adjoint which is at the same time the discrete adjoint of the discrete forward model. Such adjoint models are not harder to code than the discrete forward model.

There are a variety of symmetry-preserving discretizations available in the literature. In [20], an exhaustive overview is given of different techniques to obtain mass- or energy-conserving methods. Typically, symmetry properties of differential operators are only automatically preserved in central-difference approximations on uniform, rectilinear grids [10]. Although finite-volume methods can be used to construct conservative discretizations for mass and momentum, it is in general not possible to also obtain energy conservation [20].

In [24, 25], a fourth-order symmetry-preserving finite-volume method is constructed using Richardson extrapolation of a second-order symmetry-preserving method [22]. The extension to collocated unstructured meshes is presented in [17], and an application can be seen in [23]. The extension to upwind discretizations was made in [21], and a discretization for the convective operator was found in [9]. In [10], the method is extended to non-uniform curvilinear structured grids by deriving a discrete product rule. Furthermore, a symmetry-preserving method that conserves mass and energy for compressible flow equations with a state equation is described in [20]. For rectilinear grids, this method works well, but it is challenging to let this method work for unstructured grids.

Another option to preserve symmetry is to use discrete filters to regularize the convective terms of the equation [18, 13]. The combination of a symmetry-preserving discretization and regularization for compressible flows is studied in [16].

Mimetic finite-difference methods also mimic the important properties of differential operators. An interesting review is given in [14], and recently, a second-order mimetic discretization of the Navier-Stokes equations conserving mass, momentum, and kinetic energy was presented in [15]. The mimetic finite-difference method uses algebraic topology to design and analyze compatible discrete operators corresponding to a continuous formulation [2, 11]. In order to construct a discrete de Rham complex, certain conditions on reconstruction and reduction operators are imposed: they should be conforming, which means that the reconstruction is a right inverse of the reduction [2], they should be constant preserving [4], and the interpolation operator should commute with the differential operator [4]. In [5] a nice overview of mimetic methods is given. Discrete exterior calculus (DEC) is also related to these mimetic approaches [6].

The above papers all have their own advantages and disadvantages. In general, they are not applicable for all orders, operators, and meshes. The current paper presents a new discretization method that can handle these requirements simultaneously.

In this work, we present a new symmetry-preserving discretization of arbitrary order on curvilinear structured grids. The key idea is to use mutually-adjoint sampling and interpolation operators to switch between the continuous and discrete operator. The novelty of this work is that it combines three important requirements for discretizations: first, the symmetry-preserving discretization is made for arbitrary order of accuracy; second, the method works for every structured curvilinear mesh; and third, the method can be applied to every continuous operator. This paper is the first in a series of papers that gradually extends the theory to a general approach.

The outline of this paper is as follows: in Section 2, we present the relevant background information on positivity and symmetry, and in Section 3, we introduce our new symmetry-preserving discretization. The effectivity of this new method is presented in Section 4 for the wave equation. We conclude with a discussion of our method and future work in Section 5.

2 Background

Before presenting our new symmetry-preserving discretization, a short discussion is needed about the definitions we use for positiveness and symmetry preservation.

2.1 Inner products and positivity

In the linear space of continuous, square-integrable functions in a domain D , the standard scalar product is

$$\langle f, g \rangle = \int_D f(\vec{x})^T g(\vec{x}) \, dD.$$

In finite-dimensional spaces, any scalar product has to be given by

$$\langle x, y \rangle = x^T \mathbf{Q} y \tag{1}$$

for a matrix \mathbf{Q} which is symmetric and positive definite with respect to the standard scalar product.

Let us define operator \mathcal{A} , having domain V and co-domain W : if $x \in V$, then the *image* $\mathcal{A}x \in W$. Operators for which the domain and codomain are the same ($W = V$) are called *square*: they images 'live' in the same space as the arguments. Only square operators can be positive or negative (definite).

We distinguish the following categories:

nonnegative:	$\langle x, \mathcal{A}x \rangle \geq 0$	for all x in V ,
positive:	$\langle x, \mathcal{A}x \rangle > 0$	for all $x \neq 0$ in V ,
positive definite:	$\epsilon > 0$ exists so that $\langle x, \mathcal{A}x \rangle \geq \epsilon \langle x, x \rangle \geq 0$	for all x in V ,

and similarly, nonpositive and negative (definite) operators are defined. Note that all positive definite operators are positive, and all positive operators are nonnegative.

In finite-dimensional spaces, every positive operator is also positive definite. Nonnegative operators which are not positive must be singular: they must have a non-empty null space.

2.2 Adjoint operators and symmetry

The words adjoint and transpose are often used interchangeably. In many cases, the difference between the transpose and the adjoint is not important, but in the case of symmetry preservation, we have to specify the notion of adjoint operators a little more precisely.

The definition of the adjoint always depends on the definitions of the inner product $\langle \cdot, \cdot \rangle_V$ for the domain, and the inner product $\langle \cdot, \cdot \rangle_W$ for the codomain of the operator \mathcal{A} . The *adjoint* \mathcal{A}^* of the operator \mathcal{A} is the unique operator for which

$$\langle y, \mathcal{A}x \rangle_W = \langle \mathcal{A}^* y, x \rangle_V \quad \text{for all } x \text{ in } V \text{ and all } y \text{ in } W. \tag{2}$$

In finite-dimensional, real spaces $V = \mathbb{R}^n$, when using the standard scalar product $\langle x, y \rangle = x^T y$, the adjoint of a matrix is its transpose: $A^* = A^T$.

If the forward and adjoint operators are the same ($\mathcal{A}^* = \mathcal{A}$), we call the operator \mathcal{A} *symmetric*; if they are each other's opposites ($\mathcal{A}^* = -\mathcal{A}$), the operator is called *skew-symmetric*.

3 Symmetry-preserving discretizations

In this section, we propose a simple strategy for the construction of symmetry-preserving calculations for any differential operator \mathcal{A} . Let \mathcal{J}_p be an interpolation operator that maps from the discrete field to the continuous field, and \mathcal{S}_p be the sampling operator that produces discrete values from a continuous function [26]. We shall write the interpolated fields using italic letters and sampled fields with bold-faced letters, for example, $f := \mathcal{J}_p \mathbf{f}$, and $\mathbf{g} = \mathcal{S}_p g$.

The continuous operator \mathcal{A} is applied to the continuous field obtained from interpolation of the discrete field using \mathcal{J}_p , and the result is mapped back using \mathcal{S}_p , which leads to the discrete operator $\mathbf{A} := \mathcal{S}_p \mathcal{A} \mathcal{J}_p$.

Definition 1. The sampling operator and the interpolation operator are called *mutually adjoint* if $\mathcal{S}_p = \mathcal{J}_p^*$.

Mutual adjointness of the sampling and interpolation operator means that when the inner product of a continuous field f and a sampled field \mathbf{g} is calculated, it does not matter whether the sampled field is interpolated and the continuous inner product is used, or whether the continuous field is sampled and the discrete inner product is used: the result is the same.

Lemma 1. *Let $\mathbf{f} = \mathcal{J}_p f$ and $\mathbf{g} = \mathcal{J}_p g$. If the sampling operator and the interpolation operator are mutually adjoint, then the inner products in the discrete and continuous spaces are the same:*

$$\langle \mathbf{A}^* \mathbf{f}, \mathbf{g} \rangle_{\mathbf{P}} = \langle \mathbf{f}, \mathbf{A} \mathbf{g} \rangle_{\mathbf{P}} = \langle f, \mathcal{A} g \rangle_p = \langle \mathcal{A}^* f, g \rangle_p,$$

and the symmetry properties of \mathcal{A} will be preserved in the discretization \mathbf{A} .

Moreover, when $\langle f, f \rangle_p \geq \epsilon \langle \mathbf{f}, \mathbf{f} \rangle_{\mathbf{P}}$, then \mathbf{A} will also inherit all positiveness properties from \mathcal{A} .

Proof. When we apply the mutual adjointness of \mathcal{S}_p and \mathcal{J}_p and definition (2), we find

$$\begin{aligned} \langle \mathbf{f}, \mathbf{A} \mathbf{g} \rangle_{\mathbf{P}} &= \langle \mathbf{A}^* \mathbf{f}, \mathbf{g} \rangle_{\mathbf{P}} = \langle (\mathcal{S}_p \mathcal{A} \mathcal{J}_p)^* \mathbf{f}, \mathbf{g} \rangle_{\mathbf{P}} = \langle (\mathcal{J}_p^* \mathcal{A} \mathcal{J}_p)^* \mathbf{f}, \mathbf{g} \rangle_{\mathbf{P}} \\ &= \langle \mathbf{f}, \mathcal{J}_p^* \mathcal{A} \mathcal{J}_p \mathbf{g} \rangle_{\mathbf{P}} = \langle \mathcal{J}_p \mathbf{f}, \mathcal{A} \mathcal{J}_p \mathbf{g} \rangle_{\mathbf{P}} = \langle f, \mathcal{A} g \rangle_p = \langle \mathcal{A}^* f, g \rangle_p. \end{aligned}$$

For the second statement, we assume that \mathcal{A} is positive definite. Then

$$\langle \mathbf{f}, \mathbf{A} \mathbf{f} \rangle_{\mathbf{P}} = \langle \mathbf{f}, \mathcal{S}_p \mathcal{A} \mathcal{J}_p \mathbf{f} \rangle_{\mathbf{P}} = \langle \mathcal{J}_p \mathbf{f}, \mathcal{A} \mathcal{J}_p \mathbf{f} \rangle_p = \langle f, \mathcal{A} f \rangle_p \geq \epsilon_1 \langle f, f \rangle_p \geq \epsilon_2 \langle \mathbf{f}, \mathbf{f} \rangle_{\mathbf{P}} :$$

\mathbf{A} is positive definite as well. □

To see what the mutual adjointness actually means for the sampling and interpolation operators, they are both written in a more explicit form [26]:

$$(\mathcal{J}_p \mathbf{g})(\vec{x}) = \sum_i \mathbf{g}_i w_i(\vec{x}) \quad , \quad (\mathcal{S}_p f)_i = \int_V f(\vec{x}) s_i(\vec{x}) \, dV. \quad (3)$$

Here, w_i are the interpolation base functions, and s_i are the sampling functions. The integral of the sampling function should be 1, because that means that the sampling of a constant field is exact.

Lemma 2. *Mutual adjointness of the interpolation and sampling operators is equivalent to the following definition of the interpolation function:*

$$w_i(\vec{x}) = \sum_j s_j(\vec{x}) \mathbf{Q}_{ij}, \quad (4)$$

which means that interpolation functions can be computed if the sampling functions are chosen.

In equation (4), \mathbf{Q} is the matrix belonging to the discrete inner product (equation (1)).

Proof. Mutual adjointness of the interpolation and sampling operator means that

$$\langle f, \mathcal{J}_p \mathbf{g} \rangle_p = \langle \mathcal{S}_p f, \mathbf{g} \rangle_{\mathbf{P}}.$$

Here,

$$\langle f, \mathcal{J}_p \mathbf{g} \rangle_p = \int_V \sum_i w_i(\vec{x}) \mathbf{g}_i f(\vec{x}) dV,$$

and, since \mathbf{Q} is symmetric, we find

$$\langle \mathcal{S}_p f, \mathbf{g} \rangle_p = \sum_j \sum_i (\mathcal{S}_p f)_j \mathbf{Q}_{ji} \mathbf{g}_i = \sum_i \sum_j \left(\int_V s_j(\vec{x}) f(\vec{x}) dV \right) \mathbf{Q}_{ij} \mathbf{g}_i = \int_V \sum_i \mathbf{g}_i \sum_j s_j(\vec{x}) \mathbf{Q}_{ij} f(\vec{x}) dV,$$

such that the condition $\langle f, \mathcal{J}_p \mathbf{g} \rangle_p = \langle \mathcal{S}_p f, \mathbf{g} \rangle_p$ results in $w_i(\vec{x}) = \sum_j s_j(\vec{x}) \mathbf{Q}_{ij}$. □

If the integration matrix \mathbf{Q} had off-diagonal elements, this would mean that the interpolation base functions w become the linear combination of multiple sampling functions. Since we wish both the sampling and interpolation base functions to be zero except in a small region near a grid point, it makes no sense that the interpolation base function should be nonzero in a larger region than the sampling function. Therefore, we shall expect the integration matrix \mathbf{Q} to be a diagonal matrix. From here on, we will, therefore, use the notation $\text{diag}(\mathbf{Q})$ for the integration matrix, and the matrix entries \mathbf{Q}_i need only one row/column index. The interpolation base functions become scaled versions of the sample functions:

$$w_i(\vec{x}) = \mathbf{Q}_i s_i(\vec{x}).$$

Since $\int_V s_j(\vec{x}) dV = 1$, we find that $\mathbf{Q}_i = \int_{V_i} w_i(\vec{x}) dV$. Now that \mathbf{Q} is diagonal, we can easily choose the interpolation functions and compute the corresponding sampling functions.

3.1 Interpolation functions on a uniform 1D grid

The simplest set of interpolation base functions is the case of an infinite, uniform one-dimensional grid with unit grid distance $\Delta x = 1$. In such a case, only one base function is enough to construct all the other ones, because they are found by translation: $w_j(x) = w_0(x - j)$. The rest of this Section describes a method for the construction of the interpolation spline w_0 .

To obtain a unique spline, the following parameters are chosen:

nSpan: the span of the function's support: $w_j(x) = 0$ for all $x < j - \text{nSpan}$ and for all $x > j + \text{nSpan}$;

nCont: the number of continuous derivatives of the interpolation spline (internally), and the number of zero derivatives of the spline at the boundaries;

Order: the spline is a piecewise polynomial of order **Order**;

This parameter is not very important: for sufficiently large orders, the interpolation base function no longer depends on it.

nConsist: interpolation of all polynomials up to order **nConsist** will be exact, and the interpolation will converge with order **nConsist**;

wmax: largest grid wavenumber for which the interpolation of the function $f(x) = \exp(ix \text{wmax})$ is accurate.

The combination of linear constraints (**nCont**, **nConsist**) and linear least squares equations (**wmax**) leads to a unique set of interpolation base functions. The interpolation obtained has a formal order of accuracy given by **nConsist**, and will be accurate for grid wavenumbers up to the given maximum.

In Table 1, the parameter choices for three different interpolation splines are given. These splines are used for the computations in the rest of this paper.

Examples of interpolation base functions are shown in Figure 1. The grid wavenumber ω corresponds to the number of grid points per wavelength in the grid [8, 12]. For a given problem, which has a given Fourier spectrum, refining the grid has the effect of reducing the grid wavenumber. A sufficiently accurate solution will be found when the interpolation errors for all relevant grid

Table 1: Parameters for three different interpolation splines that are used in the rest of this paper. The three splines all satisfy $nSpan = 3$, $nCont = 1$, $Order = 11$.

	coarse	medium	fine
wmax	0.9	0.6	0.5
nConsist	3	3	4

wavenumbers are small. Therefore, Figure 1(b) illustrates how the accuracy of the interpolations may be tuned for a specific problem. We discuss two possible scenarios:

- **Modest accuracy: low convergence order**

In the first example, it will be assumed that an accuracy of 0.01% is required. Figure 1(b) shows an interpolation of third order accuracy, that is sufficiently accurate for grid wavenumbers up to 0.28π . The interpolation of fourth order accuracy requires refinement of the grid until grid wavenumbers are below 0.21π . With the lower-order interpolation, 36% fewer grid points are needed in each direction.

- **Very accurate: high convergence order**

For an accuracy of 0.002%, the 4th order interpolation allows grid wavenumbers up to 0.18π , while the lower-order interpolation needs refinement until grid wavenumbers are below 0.04π . In this case, the higher-order interpolation requires 4.5 times fewer grid points in each direction than the lower-order interpolation.

The error in $\omega = 0$ always equals zero. The number of zero derivatives in $\omega = 0$ is equal to the convergence order of the interpolation spline, so for a very accurate solution, an interpolation is needed that has the largest possible order of convergence.

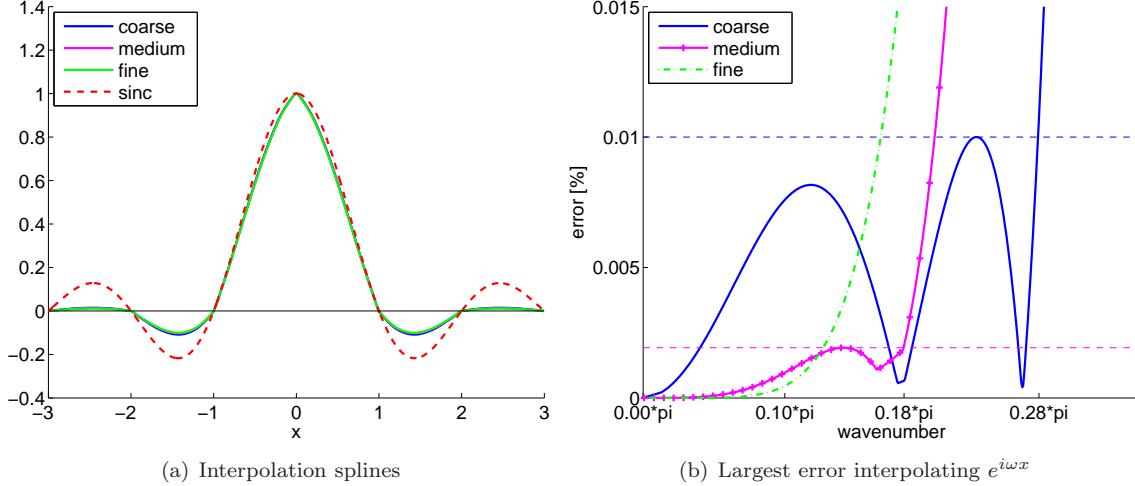


Figure 1: Interpolation base functions belonging to $nSpan=3$, $nCont=1$, $Order=11$, for different values of $wmax$ and $nConsist$. The base function is compared to the `sinc` function, which has all desired properties, but has infinite support. At the right, the largest interpolation errors over the domain are shown.

3.2 Interpolation on structured, nonlinear 3D grids

When using structured, nonlinear three-dimensional grids, we assume that some mapping exists between the (x, y, z) -locations of the physical domain and the (ξ, η, ζ) -locations in a domain which

we shall call *array space*. The physical domain points are found from the array-space locations by applying functions:

$$\begin{pmatrix} x(\xi, \eta, \zeta) \\ y(\xi, \eta, \zeta) \\ z(\xi, \eta, \zeta) \end{pmatrix} = \vec{x}(\xi, \eta, \zeta) = \vec{x}(\vec{\xi}).$$

The function $\vec{x}(\ast)$ is assumed to be 'reasonably smooth'. The grid points are found by entering integer values for the array-space coordinates ξ , η and ζ :

$$\vec{x}_{ijk} := \vec{x}(i, j, k).$$

The base function for uniform 1D grids calculated in Section 3.1 is now combined into interpolation base functions and sampling functions according to

$$w_{ijk}(\vec{x}(\xi, \eta, \zeta)) := w_0(\xi - i)w_0(\eta - j)w_0(\zeta - k),$$

$$s_{ijk}(\vec{x}) := \frac{w_{ijk}(\vec{x})}{\int_V w_{ijk}(\vec{x}) \, dV}.$$

This choice of the interpolation base functions secures the exact interpolation of constant fields, which is essential in the proof of discrete mass conservation in the example of Section 4.

The diagonal integration matrix \mathbf{Q} is given by

$$\mathbf{Q}_{ijk} := \int_V w_{ijk}(\vec{x}) \, dV.$$

4 Example: wave equation

In this section, we show the effectivity of our new method by investigating the wave equation.

4.1 The wave equation and its symmetry

A simple illustration of the effects of symmetry preservation involves the wave equation:

$$\frac{\partial^2 p}{\partial t^2} = \nabla^2 p, \tag{5}$$

where $p(\vec{x}, t)$ is the pressure. Initial conditions for p and $\partial p/\partial t$ as well as one boundary condition are needed to determine a solution of the wave equation. Mass conservation requires initial conditions for $\partial p/\partial t$ that cause the initial time derivative of mass to be zero. Therefore, we consider only initial conditions for the time derivative with a zero integral

$$\int_V \frac{\partial p}{\partial t}(\vec{x}, 0) \, dV = 0.$$

The solution of the wave equation should conserve at least two quantities: the mass M and the energy E , given by

$$M(t) := \int_V p(\vec{x}, t) \, dV \quad , \quad E(t) := \frac{1}{2} \int_V \left(\left(\frac{\partial p}{\partial t} \right)^2 + |\nabla p|^2 \right) \, dV.$$

Mass and energy are conserved in the sense that any changes over time can be expressed as the result of boundary terms called *fluxes*. Using the divergence theorem, the change in energy is given in terms of energy fluxes:

$$\begin{aligned} E'(t) &= \int_V \left(\frac{\partial^2 p}{\partial t^2} \frac{\partial p}{\partial t} + \nabla p \cdot \nabla \frac{\partial p}{\partial t} \right) \, dV = \int_V \left(\nabla^2 p \frac{\partial p}{\partial t} + \nabla p \cdot \nabla \frac{\partial p}{\partial t} \right) \, dV \\ &= \int_V \nabla \cdot \left(\nabla p \frac{\partial p}{\partial t} \right) \, dV = \oint_{\delta V} \left(\nabla p \frac{\partial p}{\partial t} \right) \cdot \vec{n} \, dS. \end{aligned}$$

In formulation (5) of the wave equation, it is not the first but the second-order time derivative of the mass that can be expressed in terms of *mass fluxes*:

$$M''(t) = \int_V \frac{\partial^2 p}{\partial t^2} dV = \int_V \nabla^2 p dV = \oint_{\delta V} \nabla p \cdot \vec{n} dS.$$

A consequence of these expressions of the time derivatives of mass and energy is that the energy and mass remain unchanged in unbounded or periodical domains.

Especially the case of energy conservation is interesting, because the expression used for the energy contains a norm of the solution. Hence, energy conservation means that the norm of the solution remains constant, which implies stability of the solution: energy conservation implies stability.

Conservation of mass and energy can also be proven using adjoints and symmetry. To do this, we write mass and energy as scalar products:

$$M(t) = \langle \mathbf{1}, p \rangle_p \quad , \quad E(t) = \frac{1}{2} \left\langle \frac{\partial p}{\partial t}, \frac{\partial p}{\partial t} \right\rangle_p + \frac{1}{2} \langle \nabla p, \nabla p \rangle_p.$$

In periodic domains, the divergence and the negative gradient are mutually adjoint ($(\nabla \cdot)^* = -\nabla$) [7], and so we get

$$\begin{aligned} E'(t) &= \left\langle \frac{\partial p}{\partial t}, \nabla \cdot \nabla p \right\rangle_p + \left\langle \nabla p, \nabla \frac{\partial p}{\partial t} \right\rangle_p = - \left\langle \nabla \frac{\partial p}{\partial t}, \nabla p \right\rangle_p + \left\langle \nabla p, \nabla \frac{\partial p}{\partial t} \right\rangle_p = 0, \\ M''(t) &= \langle \mathbf{1}, \nabla^2 p \rangle_p = - \langle \nabla \mathbf{1}, \nabla p \rangle_p = 0. \end{aligned}$$

4.2 Discrete model

In the discrete case, we have precisely the same results. The discrete wave equation will be given by

$$\mathbf{p}''(t) = \mathbf{A} \mathbf{p} =: \mathcal{S}_p \nabla^2 \mathcal{J}_p \mathbf{p}.$$

Discrete mass M and energy E will be given by

$$M(t) := \langle \mathbf{1}, \mathbf{p} \rangle_p \quad , \quad E(t) := \frac{1}{2} \langle \mathbf{p}', \mathbf{p}' \rangle_p - \frac{1}{2} \langle \mathbf{p}, \mathbf{A} \mathbf{p} \rangle_p.$$

and their time derivatives are zero, using the same steps as in the continuous proof, and the mutual adjointness of the sampling and interpolation operator:

$$\begin{aligned} M''(t) &:= \langle \mathbf{1}, \mathbf{A} \mathbf{p} \rangle_p = \langle \mathbf{1}, \mathcal{S}_p \nabla^2 \mathcal{J}_p \mathbf{p} \rangle_p = \langle \mathcal{J}_p \mathbf{1}, \nabla^2 \mathcal{J}_p \mathbf{p} \rangle_p = - \langle \nabla \mathbf{1}, \nabla \mathcal{J}_p \mathbf{p} \rangle_p = 0. \\ E'(t) &:= \langle \mathbf{p}', \mathbf{A} \mathbf{p} \rangle_p - \langle \mathbf{p}, \mathbf{A} \mathbf{p}' \rangle_p = 0. \end{aligned}$$

The proof of mass conservation requires the perfect interpolation of the constant field: $\mathcal{J}_p \mathbf{1} = \mathbf{1}$.

4.3 Numerical results

The wave equation is discretized on a uniform and a 2D curvilinear grid for the unit square with periodic boundaries, shown in Figure 2. This results in the following equation: $\mathbf{p}'' = \mathbf{A} \mathbf{p}$, where \mathbf{A} is given by $\mathbf{A} = \mathcal{S}_p \nabla^2 \mathcal{J}_p$, and definition (3) is applied. Note that the discretization matrix \mathbf{A} belonging to the wave equation is negative definite, and hence, it has negative eigenvalues.

A Runge-Kutta time-integration method is used, where it is verified that the time integration is accurate enough such that it has no influence on the results. The initial conditions are chosen such that the exact solution is a one-dimensional, traveling Gaussian wave, given by

$$p_{exact}(x, y, t) = \exp \left(- \left(\frac{\text{mod} \left(x - y - t\sqrt{2} + \frac{1}{2}, 1 \right) - \frac{1}{2}}{\sqrt{0.03}} \right)^2 \right).$$

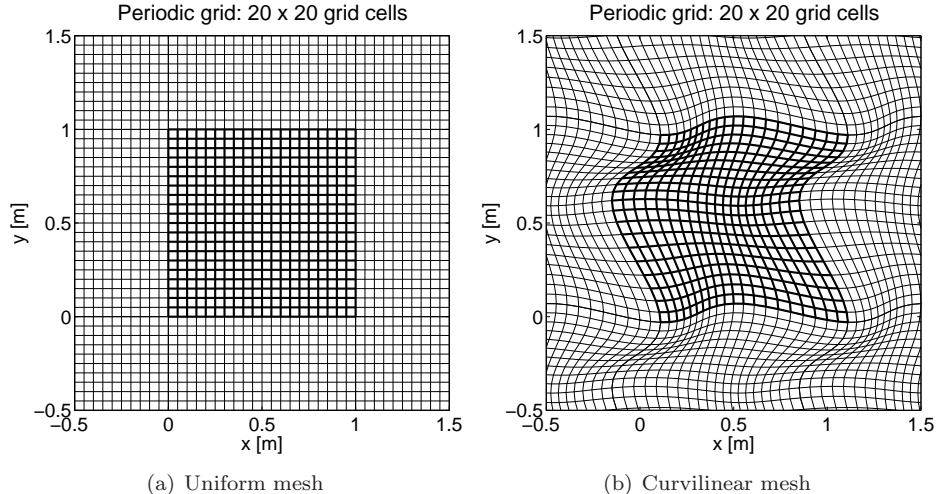


Figure 2: 2D grid on $[0, 1] \times [0, 1]$ used for the discretization of the wave equation. An impression of the periodicity is given by extending the mesh on each boundary.

The exact solution is sampled directly to obtain a reference solution:

$$(\mathbf{p}_{ref}(t))_{ij} := p_{exact}(x_{ij}, y_{ij}, t).$$

Initial conditions for \mathbf{p} and \mathbf{p}' are taken from the reference solution, but a correction is applied to the time derivative \mathbf{p}' :

$$\mathbf{p}_0 := \mathbf{p}_{ref}(0) \quad , \quad \mathbf{p}'_0 := (\mathbf{I} - \mathbf{b}\mathbf{b}^T \text{diag}(\mathbf{Q})) \mathbf{p}'_{ref}(0),$$

where $\mathbf{b}_i = 1 \forall i$. This choice for $\mathbf{p}'(0)$ makes sure that $\mathbf{M}'(0) = \mathbf{b}^T \text{diag}(\mathbf{Q}) \mathbf{p}'(0) = 0$.

The relative root-mean-square error over time for the approximation on the uniform and curvilinear mesh are given in Table 2. For each choice of interpolation spline, the best choice of mesh is emphasized in bold. As expected, the coarse interpolation results in the most accurate approximations if the mesh is coarse, and the fine interpolation when the grid is fine. The medium interpolation is most accurate when the grid is between coarse and fine.

The errors increase slightly when time grows. However, the error percentages are still small enough to trust the approximation. Though the errors decrease rapidly with refinement of the mesh, the results do not show a clear rate of convergence. This is typical for the type of interpolation used.

Table 3 shows the loss of mass and energy during the simulation with the medium interpolation method on a 20×20 uniform and curvilinear mesh. Though the accuracy is limited in this case (errors up to 4.47% for the uniform mesh), the mass and energy losses are negligible up to machine accuracy. This is due to the symmetry-preserving nature of the discretization, and is true for all the simulations.

The results show that the method succeeds in constructing a symmetry-preserving discretization on a curvilinear, structured mesh.

5 Conclusion

This paper describes a simple and effective strategy for the construction of symmetry-preserving methods on curvilinear, structured grids, offering flexibility and accuracy of the numerical approximations. The key idea is to use mutually-adjoint interpolation and sampling operators to switch from the continuous to the discrete operator. The numerical example shows that the method leads

Table 2: Relative root-mean-square error (in percentages) of the approximation for different interpolation splines (taken from Table 1) and mesh sizes. For each choice of interpolation spline, the best choice of mesh is emphasized in bold.

Uniform mesh on $[0, 1] \times [0, 1]$									
Time	Coarse interpolation			Medium interpolation			Fine interpolation		
	20x20	40x40	80x80	20x20	40x40	80x80	20x20	40x40	80x80
1	0.30%	0.056%	0.023%	0.64%	0.011%	0.0042%	0.85%	0.018%	0.00045%
2	0.59%	0.111%	0.045%	1.24%	0.020%	0.0055%	1.66%	0.032%	0.00057%
3	0.86%	0.171%	0.070%	1.81%	0.025%	0.0053%	2.41%	0.052%	0.00061%
4	1.11%	0.223%	0.091%	2.32%	0.036%	0.0070%	3.11%	0.063%	0.00057%
5	1.33%	0.276%	0.113%	2.75%	0.042%	0.0066%	3.70%	0.081%	0.00051%
6	1.53%	0.335%	0.137%	3.14%	0.050%	0.0071%	4.27%	0.096%	0.00041%
7	1.71%	0.390%	0.160%	3.46%	0.059%	0.0088%	4.76%	0.113%	0.00058%
8	1.84%	0.447%	0.183%	3.80%	0.067%	0.0104%	5.32%	0.127%	0.00060%
9	1.94%	0.507%	0.208%	4.11%	0.073%	0.0101%	5.86%	0.146%	0.00070%
10	2.00%	0.557%	0.228%	4.47%	0.085%	0.0124%	6.48%	0.160%	0.00064%

Curvilinear mesh on $[0, 1] \times [0, 1]$									
Time	Coarse interpolation			Medium interpolation			Fine interpolation		
	20x20	40x40	80x80	20x20	40x40	80x80	20x20	40x40	80x80
1	2.3%	0.052%	0.024%	2.9%	0.052%	0.0045%	3.2%	0.079%	0.0044%
2	3.7%	0.098%	0.048%	4.8%	0.093%	0.0062%	5.4%	0.149%	0.0053%
3	4.9%	0.139%	0.070%	6.5%	0.119%	0.0071%	7.4%	0.207%	0.0055%
4	6.9%	0.191%	0.097%	9.1%	0.168%	0.0105%	10.1%	0.286%	0.0081%
5	7.5%	0.228%	0.119%	10.0%	0.203%	0.0119%	11.1%	0.354%	0.0085%
6	9.4%	0.282%	0.145%	12.2%	0.251%	0.0147%	13.5%	0.432%	0.0108%
7	0.2%	0.328%	0.169%	12.7%	0.289%	0.0165%	13.7%	0.497%	0.0118%
8	0.6%	0.366%	0.188%	13.0%	0.315%	0.0179%	13.9%	0.559%	0.0120%
9	2.6%	0.425%	0.219%	14.6%	0.373%	0.0210%	15.4%	0.645%	0.0146%
10	1.8%	0.455%	0.237%	12.7%	0.388%	0.0225%	13.0%	0.686%	0.0147%

Table 3: Percentage of mass and energy loss in the approximation on a 20×20 (coarse) mesh, using an interpolation spline with parameters `nSpan = 3`, `nCont = 1`, `Order = 11`, `nConsist = 3`, `wmax = 0.6` (medium interpolation).

Time	Uniform mesh		Curvilinear mesh	
	Mass loss	Energy loss	Mass loss	Energy loss
1	3.5E-08%	1.8E-11%	3.9E-07%	1.5E-12%
2	7.0E-08%	2.5E-11%	8.3E-07%	2.2E-12%
3	1.0E-07%	3.2E-11%	1.1E-06%	2.9E-12%
4	1.4E-07%	3.8E-11%	1.6E-06%	3.8E-12%
5	1.7E-07%	4.2E-11%	1.9E-06%	4.9E-12%
6	2.1E-07%	4.4E-11%	2.4E-06%	6.0E-12%
7	2.4E-07%	4.8E-11%	2.8E-06%	7.0E-12%
8	2.8E-07%	5.2E-11%	3.1E-06%	8.1E-12%
9	3.1E-07%	5.6E-11%	3.6E-06%	9.2E-12%
10	3.4E-07%	6.1E-11%	3.9E-06%	1.0E-11%

to results in which a high accuracy can be obtained, while the discrete mass and energy are both preserved.

The simulation of flow phenomena typically uses staggered grids, in which scalar fields and vector field components each have their own grids, and where each grid is shifted half a grid size with respect

to the other grids. Applying the discretization strategy explained in this paper is possible on such grids, but the details are outside the scope of this paper and will be the subject of a next paper.

One area of concern might be the number of non-zero elements in the discretization matrix. In a 3D calculation, any interpolation that is nonzero in a certain block results in a nonzero in the discretization matrix. Therefore, the number of nonzeros on every row will be $(4 * nSpan - 1)^3$. The reduction of this number of nonzeros for each row will be discussed in another paper.

Finally, future work includes handling local grid refinements and the symmetry-preserving treatment of the compressible flow equations.

Acknowledgments

The authors gratefully wish to acknowledge the useful comments provided by Marc Gerritsma and Artur Palha from TU Delft and Eric Duvebeck from Shell that helped to shape this work. We also thank VORtech and Shell that allowed us to develop this work.

References

- [1] G.A. Blaisdell, E.T. Spyropoulos, and J.H. Qin. The effect of the formulation of nonlinear terms on aliasing errors in spectral methods. *Applied Numerical Mathematics*, 21:207–219, 1996.
- [2] P.B. Bochev and J.M. Hyman. Principles of Mimetic Discretizations of Differential Operators. In D.N. Arnold, P.B. Bochev, R.B. Lehoucq, R.A. Nicolaides, and M. Shashkov, editors, *Compatible Spatial Discretizations*, volume 142 of *The IMA Volumes in Mathematics and its Applications*, pages 89–119. Springer New York, 2006.
- [3] A.M. Bradley. PDE-constrained optimization and the adjoint method, 2013.
- [4] F. Brezzi and A. Buffa. Innovative mimetic discretizations for electromagnetic problems. *Journal of Computational and Applied Mathematics*, 234(6):1980–1987, 2010.
- [5] F. Brezzi, A. Buffa, and G. Manzini. Mimetic scalar products of discrete differential forms. *Journal of Computational Physics*, 257:1228–1259, 2014.
- [6] A.N. Hirani. *Discrete Exterior Calculus*. PhD thesis, California Institute of Technology, 2003.
- [7] J.M. Hyman and M. Shashkov. Adjoint operators for the natural discretizations of the divergence, gradient and curl on logically rectangular grids. *Applied Numerical Mathematics*, 25:413–442, 1997.
- [8] J.W. Kim and D.J. Lee. Optimized Compact Finite Difference Schemes with Maximum Resolution. *AIAA Journal*, 34:887–893, 1996.
- [9] J.C. Kok. A symmetry and dispersion-relation preserving high-order scheme for aeroacoustics and aerodynamics. Technical Report NLR-TP-2006-525, National Aerospace Laboratory NLR, 2006.
- [10] J.C. Kok. A high-order low-dispersion symmetry-preserving finite-volume method for compressible flow on curvilinear grids. *Journal of Computational Physics*, 228:6811–6832, 2009.
- [11] J. Kreeft, A. Palha, and M. Gerritsma. Mimetic framework on curvilinear quadrilaterals of arbitrary order, 2011. arXiv:1111.4304.
- [12] Y.-H. Kuo, L. Lee, and G. Lyng. Analysis and development of compact finite difference schemes with optimized numerical dispersion relations, 2014. arXiv:1409.3535.
- [13] O. Lehmkuhl, R. Borrell, I. Rodríguez, C.D. Pérez-Segarra, and A. Oliva. Assessment of the symmetry-preserving regularization model on complex flows using unstructured grids. *Computers & Fluids*, 60:108–116, 2012.

- [14] K. Lipnikov, G. Manzini, and M. Shashkov. Mimetic finite difference method. *Journal of Computational Physics*, 257:1163–1227, 2014.
- [15] G.T. Oud, D.R. van der Heul, C. Vuik, and R.A.W.M. Henkes. A fully conservative mimetic discretization of the Navier-Stokes equations in cylindrical coordinates with associated singularity treatment. *Journal of Computational Physics*, 325:314–337, 2016.
- [16] W. Rozema, R.W.C.P. Verstappen, J.C. Kok, and A.E.P. Veldman. A Symmetry-Preserving Discretization and Regularization Subgrid Model for Compressible Turbulent Flow. In J. Fröhlich, H. Kuerten, B.J. Geurts, and V. Armenio, editors, *Direct and Large-Eddy Simulation IX*, volume 20 of *ERCOTAC Series*, pages 319–325, 2015.
- [17] F.X. Trias, O. Lehmkuhl, A. Oliva, C.D. Pérez-Segarra, and R.W.C.P. Verstappen. Symmetry-preserving discretization of Navier-Stokes equations on collocated unstructured grids. *Journal of Computational Physics*, 258:246–267, 2014.
- [18] F.X. Trias and R.W.C.P. Verstappen. On the construction of discrete filters for symmetry-preserving regularization models. *Computers & Fluids*, 40:139–148, 2011.
- [19] J. Tromp, C. Tape, and Q. Liu. Seismic tomography, adjoint methods, time reversal and banana-doughnut kernels. *Geophysical Journal International*, 160:195–216, 2005.
- [20] B. van 't Hof and A.E.P. Veldman. Mass, momentum and energy conserving (MaMEC) discretizations on general grids for the compressible Euler and shallow water equations. *Journal of Computational Physics*, 231:4723–4744, 2012.
- [21] A.E.P. Veldman and K.-W. Lam. Symmetry-preserving upwind discretization of convection on non-uniform grids. *Applied Numerical Mathematics*, 58:1881–1891, 2008.
- [22] A.E.P. Veldman and K. Rinzema. Playing with nonuniform grids. *Journal of Engineering Mathematics*, 26:119–130, 1992.
- [23] R.W.C.P. Verstappen and R.M. van der Velde. Symmetry-preserving discretization of heat transfer in a complex turbulent flow. *Journal of Engineering Mathematics*, 54:299–318, 2006.
- [24] R.W.C.P. Verstappen and A.E.P. Veldman. Spectro-consistent discretization of Navier-Stokes: a challenge to RANS and LES. *Journal of Engineering Mathematics*, 34:163–179, 1998.
- [25] R.W.C.P. Verstappen and A.E.P. Veldman. Symmetry-preserving discretization of turbulent flow. *Journal of Computational Physics*, 187:343–368, 2003.
- [26] M. Vetterli, J. Kovačević, and V.K. Goyal. *Foundations of Signal Processing*. Cambridge University Press, 2014.